

# Stability and Response of Two-Bladed Gimballed Rotors with Coning Hinges

Giulio Avanzini\*

Università del Salento, 72100 Brindisi, Italy

Guido De Matteis†

“Sapienza” Università di Roma, Rome, 00184, Italy

and

Alberto Torasso‡

Politecnico di Torino, Turin, 10129, Italy

## Abstract

This paper aims to analyze the characteristics of a two-bladed gimballed rotor featuring a homokinetic joint between driving shaft and rotor yoke and a fly-bar with paddles. Blades are connected to the yoke by coning hinges. A pitch-coning link is introduced for gust load alleviation.

The design and testing of this rotor configuration is part of the development program of a lightweight helicopter in the VLR rotorcraft certification framework. The rotor is designed with the main objective of solving some of the negative issues that affect the use of teetering rotors on light helicopters, such as strong 2/rev oscillatory loads, poor response at low  $g$ 's and a pronounced sensitivity to gusts and/or large pilot inputs.

The work is focused on stability issues related to the presence of coning hinges and their effects on rotor response and loads transmitted to the hub, affected by the variation of mass properties associated to (possibly non-symmetric) coning rotations. To this end a dynamic model is developed, that captures the most relevant aspects of the mechanical interactions between blades and yoke. Numerical simulation and stability analysis are performed to assess possible advantages of the configuration with respect to a conventional teetering rotor.

\*Professor, Faculty of Industrial Engineering, Edificio 14 Cittadella della Ricerca, S.S. 7 Km.7.3, e-mail: [giulio.avanzini@unisalento.it](mailto:giulio.avanzini@unisalento.it), tel. +39 0831 507427, fax +39 0831 507327; AIAA Senior Member.

†Professor, Dept. of Mechanical and Aerospace Engineering, Via Eudossiana 18, e-mail: [dematteis@dma.ing.uniroma1.it](mailto:dematteis@dma.ing.uniroma1.it), tel. +39 06 44585210, fax +39 06 4882576; AIAA Senior Member.

‡Ph. D. Student, Dept. of Aerospace Engineering, C.so Duca degli Abruzzi 24, e-mail: [alberto.torasso@polito.it](mailto:alberto.torasso@polito.it), tel. +39 011 5646871, fax +39 011 5646899; AIAA Member.

## Nomenclature

$c$	blade/paddle chord
$C_{L\alpha}$	lift curve slope of the blade/paddle section
$I_{bl}$	blade inertia around coning hinge
$J_{fb}$	fly-bar inertia
$J_{H_i}$	hub moments of inertia around feathering (F), polar (P) and teetering (T) axes
$K$	hub stiffness
$k_{fr}$	dry friction in coning hinge
$K_{PC}$	pitch-coning coupling
$K_T$	feathering hinge stiffness
$m_{bl}$	blade mass
$R$	blade radius
$R_{fb}$	fly-bar mean radius
$S_{bl}$	blade static inertia around coning hinge
$S_{fb}$	paddle area
<i>Greek symbols</i>	
$\alpha_g$	blade AoA variation caused by a gust
$\beta_0, \gamma$	hub flapping and feathering angles
$\beta_1, \beta_2$	coning angles
$\theta$	blade pitch angle
$\theta_0, \theta_{cyc}$	collective and cyclic pitch commands
$\theta_H, \phi_H$	longitudinal and lateral hub tilt angles
$\theta_{SW}, \phi_{SW}$	longitudinal and lateral swashplate rotations
$\lambda$	non-dimensional uniform inflow velocity
$\mu$	advance ratio
$\rho$	air density
$\psi$	blade anomaly
$\Omega$	rotor angular speed
<i>Subscripts</i>	
$bl$	blade
$C$	coning hinge
$f$	fuselage
$fb$	fly-bar
$H$	hub frame
$R$	rotating-shaft frame

## Introduction

The paper aims at providing a detailed study on the characteristics of a novel two-bladed gimballed rotor, featuring aerodynamic paddles and coning hinges, outlining possible advantages and peculiarities with respect to a more conventional teetering rotor of equivalent size, for use on a light helicopter. After a preliminary study [1] focused on the definition of a simplified model suitable for capturing the basic dynamic behaviour of a rigid two-bladed gimballed rotor and its stability, the effects of coning hinges on rotor response to commands and gust loads will be analyzed for the two classes of rotors.

The two-bladed gimballed rotor configuration discussed in the paper, featuring a fly-bar with paddles, is being considered as a possible way for alleviating some of the drawbacks that affect conventional teetering rotors. The solution here considered relies on a rigid yoke articulated with respect to the shaft by means of a spherical hinge, realized by means of a set of elastomeric springs to improve the handling qualities of the helicopter at low load factor.

Two rigid blades are connected to the hub yoke by means of coning hinges, while the fly-bar features two low-aspect-ratio paddles at the tips. From the purely mechanical standpoint, this configuration allows one more degree of freedom to the blades in the rotating frame with respect to a conventional teetering rotor, as the flapping motion around the axis perpendicular to both the shaft and blade axes is accompanied by a feathering motion around the blade axis itself, this latter rotation corresponding to the flap angle for the paddles. The actual pitch angle of each blade will thus result from the combination of the direct command, delivered by a conventional swash-plate, and the feathering motion of the rotor.

The introduction of coning hinges significantly increases model complexity with respect to the rigid gimballed rotor considered in [1], not simply because of the higher number of system degrees of freedom, but for the significant variation of rotor inertial properties associated to blade rotations around coning hinges. Both realistic coning hinges with friction induced by the centrifugal load, and ideal, frictionless ones will be considered. Finally, the presence of a pitch-coning link varies blade pitch as a function of coning angles, a feature introduced in order to alleviate gust loads which, at the same time, significantly affects system stability.

Most of the simplifying assumptions at the basis of the model derived in [2] are no longer valid, first of all the possibility of representing the gimballed rotor as a rigid body suspended to a spherical hinge. The derivation of the rotor model is carried out by means of a Newtonian approach, writing a generalized formulation for angular momentum balance, where the centre of the spherical hinge is adopted as reference pole for hub degrees of freedom dynamics, while coning hinges are considered as poles for rotor blade coning motion. When a small angle assumption is made and linear airfoil section aerodynamics is assumed, loads can be analytically integrated [3]. An 8<sup>th</sup> order linear time varying model is derived, to be compared with a fourth-order linear model discussed in [1], where a fixed coning angle was assumed, in order to assess the effects and relevance of coning dynamics on rotor response.

Following the same approach discussed in [1], a 6<sup>th</sup> order linear model of a teetering rotor with coning hinges is derived and validated against the results obtained from a fully-nonlinear model, derived by means of a Lagrangian formulation, as described in [4]. All the relevant features related to the presence of coning hinges were captured by the simple linear model, so that the development of a complex fully nonlinear model for the gimballed rotor with coning hinges was considered not necessary for the scopes of the study.

The comparison between the two different classes of rotor systems, that is, teetering and gimballed, is then carried out using the relatively simple linear periodic dynamical models, that correctly represent the effects of rotor parameter variations, and the resulting characteristics in terms of response and stability. The peculiarities and possible advantages of the gimballed rotor with respect to a more traditional teetering configuration are thus outlined.

The presence of a sustained wobbling motion is the principal characteristic of the two-bladed gimballed rotor observed in [2] and [5], a motion interpreted as the result of the difference in the tip-path-planes described by blades and paddles, for the rigid rotor case [1].

Moreover, these previous studies demonstrated how the inertial properties of the feathering axis have a marginal effect on rotor behaviour, while the presence of the paddles is necessary for stabilizing the motion and avoid the departures experienced by the rotor in the presence of periodic forcing terms. These features are basically maintained even in the presence

of coning degrees of freedom, although pitch–coning coupling significantly affects rotor stability.

In this framework, relevant differences are present with respect to three–bladed gimballed rotors featuring coning hinges, where polar symmetry of the inertia tensor gyroscopically stabilize the rotor and pitch–coning coupling only affect rotor load [6, 7]. On the converse, a coupled teetering and coning mode becomes unstable for both gimballed and teetering two–bladed rotors in the ideal case (frictionless coning hinges), for pitch–coning gains higher than a certain threshold. The introduction of coning hinges and pitch–coning coupling is also relevant to the analysis of rotor loads during gust encounters, that will be carried out in the final part of the paper.

The derivation of the equations of motion for the gimballed rotor with coning hinges, which is one of the original contributions of the paper, is reported in the next Section. On the converse, the dynamics of two–bladed gimballed rotors with fixed coning angles and teetering rotors, used for the comparisons, are introduced without derivation. Referencing to previous works provides the relevant material [1,2,3]. The third section presents the results of the analysis. It is divided into two parts: in the first one, the stability analysis is carried out and the effects of friction in the coning hinges are analyzed, whereas in the second subsection gust loads for all the considered configurations are evaluated. A section of Conclusions ends the paper.

## Rotor Models

The gimballed rotor with coning hinges features a yoke connected to the main rotor shaft through a spherical joint, that allows two relative angular degrees of freedom for feathering and teetering, indicated in Fig. 1 as  $\gamma$  and  $\beta_0$ , respectively. The blades are connected to the yoke through coning hinges, placed at a distance  $r_c$  from the rotor axis, with a geometrical undersling  $h_c$  with respect to the centre of the gimbal.

The configuration is similar, in some respect, to the teetering rotor mounted on the Robinson R-22 helicopter, with the major difference that the spherical joint replaces the teetering hinge, thus allowing one more degree of freedom to the yoke. The isolated gimballed rotor model will be compared with an equivalent teetering one in terms of dynamic behaviour and response to controls, in a way similar to

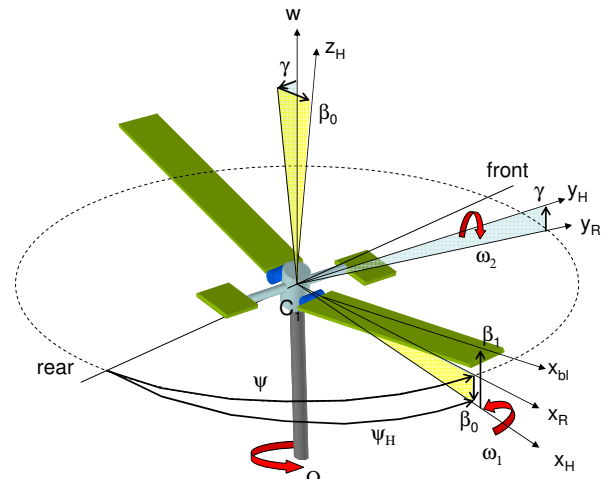


Figure 1: Rotor geometry.

that followed in [1]. A simplified helicopter model is also derived, that features a vertical translational degree of freedom only (heave motion) with uniform dynamic inflow, in order to investigate the loads transmitted during a gust encounter and the effects of the pitch–coning link.

### Equations of motion of a two–bladed gimballed rotor with coning hinges

The equations of motion of the rotor with coning hinges are obtained starting from the generalized Euler equation, that is, angular momentum balance written with respect to a pole which is displaced from the centre of mass of the system [8]. Three equations in vector form are written: one for the angular momentum balance of the whole rotor, considered as an articulated body, the attitude of which is represented by means of teetering and feathering angles ( $\beta_0$  and  $\gamma$ ) representing the inclination of the yoke with respect to the rotor shaft around the spherical gimbal; and two equations for the coning motion of each blade with respect to the yoke, represented by means of coning angles,  $\beta_i$ ,  $i = 1, 2$ .

### Hub equations

Hub motion is described using the centre of the spherical joint,  $O$ , as the pole for moments. Angular momentum balance of the entire rotor is written as

$$\frac{d\vec{h}_O}{dt} + m_{rot}\vec{r}_{CM} \times \vec{a}_O = \vec{m}_O \quad (1)$$

where external torques  $\vec{m}_O$  and angular momentum  $\vec{h}_O$  are referred to  $O$ ,  $m_{rot}\vec{r}_{CM}$  is the static moment

of the rotor,  $\mathbf{r}_{CM}$  is the position vector of rotor centre of mass with respect to  $O$  and  $\vec{\mathbf{a}}_O$  the absolute acceleration of  $O$ . The total angular momentum of the rotor with respect to  $O$  is given by

$$\vec{\mathbf{h}}_O = \mathbf{I}(\beta_1, \beta_2)\vec{\boldsymbol{\omega}} + \vec{\mathbf{h}}_1^{rel} + \vec{\mathbf{h}}_2^{rel}$$

where  $\mathbf{I}(\beta_1, \beta_2)$  is the inertia tensor which, in the most general case, depends on the time-varying coning angles,  $\beta_1$  and  $\beta_2$ , while  $\vec{\boldsymbol{\omega}}$  is the hub angular velocity. The relative angular momentum due to the motion of the  $i$ -th blade relative to a reference frame fixed to the central hub,  $\vec{\mathbf{h}}_i^{rel}$ , is expressed as

$$\vec{\mathbf{h}}_i^{rel} = \int_0^\ell \mu(x_{bl}) \left[ (\vec{\mathbf{r}}_{OC} + \vec{\mathbf{r}}_{CP}) \times \vec{\mathbf{v}}_P^{rel} \right] dx_{bl} \quad (2)$$

where  $\mu(x_{bl})$  is the linear density of the blade and

$$\vec{\mathbf{v}}_P^{rel} = \frac{d\vec{\mathbf{r}}_{CP}}{dt}$$

is the speed relative to the hub of the blade element  $\mu(x_{bl})dx$  placed in  $P$ , at a distance  $x_{bl}$  from the coning hinge along the blade span.

### Moments of Inertia

As outlined above, the inertia tensor of the rotor varies as a function of the coning angles. The inertia of the rotor is the sum of the contributions from central hub,  $\mathbf{J}_H = \text{diag}(J_{HF}, J_{HT}, J_{HP})$ , flybar  $\mathbf{J}_{fb} = \text{diag}(J_{fb}, 0, J_{fb})$ , (where the fly-bar, aligned with the teetering axis is assumed to have negligible inertia around it, its remaining moments of inertia being approximately equal) and blades. The contributions of the blades around teetering, feathering and polar axes are given respectively by

$$J_{bl_T} = 2 \{ m_{bl}(r_C^2 + h_C^2) + I_{bl} + S_{bl} [r_C(\cos \beta_1 + \cos \beta_2) + h_C(\sin \beta_1 + \sin \beta_2)] \}$$

$$J_{bl_F} = 2 [ m_{bl}h_C^2 + S_{bl}h_C(\sin \beta_1 + \sin \beta_2) ] + I_{bl}(\sin^2 \beta_1 + \sin^2 \beta_2)$$

$$J_{bl_P} = 2 [ m_{bl}r_C^2 + S_{bl}r_C(\cos \beta_1 + \cos \beta_2) ] + I_{bl}(\cos^2 \beta_1 + \cos^2 \beta_2)$$

where reference is made to the Nomenclature section for the meaning of the symbols. The blades also cause the presence of an off-diagonal term in the inertia tensor, equal to

$$J_{bl_{xz}} = S_{bl} [r_C(\sin \beta_1 - \sin \beta_2) + h_C(\cos \beta_1 + \cos \beta_2)] - I_{bl}(\sin \beta_1 \cos \beta_1 - \sin \beta_2 \cos \beta_2)$$

### Blade equations

Blade motion around its coning hinge is described by means of a vector equation formally identical to Eq. (1)

$$\frac{d\vec{\mathbf{h}}_{C,i}^{rel}}{dt} + m_{bl}\vec{\mathbf{r}}_{CG,i} \times \vec{\mathbf{a}}_{C,i} = \vec{\mathbf{m}}_{C,i} \quad (3)$$

where moments are evaluated with respect to the coning hinge,  $C_i$ , and only a single relative degree of freedom,  $\beta_i$ , is available around the hinge axes,  $\mp \hat{\mathbf{j}}$ , parallel to the  $y_H$  axis of the hub-fixed frame,  $\mathcal{F}_H$ , where the  $-$  sign is used for blade #1, placed on the positive side of the  $x_H$  axis.

The relative angular momentum of the  $i$ -th blade  $\vec{\mathbf{h}}_{C,i}^{rel}$  with respect to the hinge  $C_i$  is equal to

$$\vec{\mathbf{h}}_{C,i}^{rel} = \int_0^\ell \mu(x_{bl}) \left( \vec{\mathbf{r}}_{CP} \times \vec{\mathbf{v}}_P^{rel} \right) dx_{bl}, \quad i = 1, 2 \quad (4)$$

where  $m_{bl}\vec{\mathbf{r}}_{CG,i}$  is the static moment of the blade with respect to  $C_i$  and

$$\vec{\mathbf{a}}_{C,i} = \frac{d^2\vec{\mathbf{r}}_{OC}}{dt^2}$$

is the absolute acceleration of  $C_i$ . The relative speed  $\vec{\mathbf{v}}_P^{rel}$  of the mass element  $\mu(x_{bl})dx_{bl}$  in  $P$ , with abscissa  $x_{bl}$  counted along the blade span, is

$$\vec{\mathbf{v}}_P^{rel} = \vec{\mathbf{v}}_P - \vec{\mathbf{v}}_{C,i}.$$

### Aerodynamics

Aerodynamic moments around coning hinges,  $m_{C,i}$ ,  $i = 1, 2$ , and the corresponding torques around teetering and feathering axes,  $m_F$  e  $m_T$ , are expressed adopting an approach identical to that described in [1], with minor variations, in order to take into account the additional coning degrees of freedom. The lift of each blade is expressed as

$$L_i \approx \frac{1}{6} \rho \Omega^2 R^3 c (1 \pm 3\mu \sin \psi) C_{L_\alpha} \alpha_i, \quad i = 1, 2$$

It is assumed that  $L_i$  is applied at  $0.7R$ , where the upper and lower signs apply to the first and second blade, respectively. This convention will be adopted throughout the paper. Rotor inflow and blade drag are not included in the simplified model, as they were shown to have negligible effects on the dynamic behaviour of the gimballed rotor around the teetering and feathering axes [1]. The most relevant variation

with respect to the simplified model of [1] are (i) the pitch–coning coupling, that introduces a variation in blade pitch as a function of coning angle, and (ii) the variation of blade incidence induced by coning rates. As a consequence of this latter effect, aerodynamic damping around the teetering axis, previously expressed in the simple form  $-B\omega_2$ , is now given by  $-B[\omega_2 - \tau(\dot{\beta}_1 - \dot{\beta}_2)]$ , where  $\tau = (0.7R - r_c)/(0.7R)$ ,  $r_c$  being the eccentricity of the coning hinge.

As for coning dynamics, the aerodynamic forcing term is given by lift acting with a moment arm equal to  $0.7R - r_c$  with respect to the coning hinge. Note that in the previous work it was not necessary to express the lift of the single blade, but only the lift unbalance between the two blades of the rotor.

In the presence of a coning rate and pitch–coning coupling, the angle of attack of the reference section at  $0.7R$  is evaluated as

$$\alpha_i \approx \theta_0 \pm \theta_{cyc} \pm \omega_2/\Omega - K_{PC}\beta_i - \tau\dot{\beta}_i/\Omega + \Delta\alpha_{g_i}$$

where, together with standard control variables, namely, collective and cyclic pitch,  $\theta_0$  and  $\theta_{cyc} = -a_1 \cos \psi - b_1 \sin \psi$ , the effects of coning rate,  $\dot{\beta}_i$ , and pitch–coning coupling,  $-K_{PC}\beta_i$ , are included. Variations of angle of attack due to a vertical gust,  $\Delta\alpha_{g_i}$ , are also considered, assuming that the two blades may enter the gust at different times, so that, in general, it is  $\Delta\alpha_{g_1} \neq \Delta\alpha_{g_2}$ .

At hovering, cyclic pitch commands are close to zero and each blade provides a constant lift force equal to half of the total weight of the vehicle, such that

$$L_1 = L_2 = \frac{1}{6}\rho\Omega^2 R^3 cC_{L_\alpha}(\theta_0 - K_{PC}\beta_H) = \frac{W}{2}.$$

Coning and incidence angles can thus be expressed in the form

$$\begin{aligned} \beta_i &= \beta_H + \Delta\beta_i \\ \alpha_i &= \alpha_H + \Delta\alpha_i \end{aligned} \quad i = 1, 2$$

where

$$\Delta\alpha_i = \Delta\theta_0 \pm \theta_{cyc} \pm \omega_2/\Omega - K_{PC}\Delta\beta_i - \tau\dot{\beta}_i/\Omega + \Delta\alpha_{g_i}$$

At hovering  $\beta_i = \beta_H$  and  $\alpha_i = \alpha_H$ ,  $i = 1, 2$ . Considering flight conditions at low advance ratio  $\mu$ , the angular variables remain small and it is possible to express the lift developed by the blades in the form

$$L_i \approx \frac{W}{2}(1 \pm 3\mu \sin \psi) + \frac{1}{6}\rho\Omega^2 R^3 cC_{L_\alpha} \Delta\alpha_i$$

It is now possible to evaluate the moments acting on the elements of the gimballed rotor. Blade coning motion is driven by aerodynamic moment with respect to the coning hinge

$$m_{C_i}^{aero} = (0.7R - r_c) \times L_i$$

whereas the total moment acting on the rotor around the teetering axis passing through the centre of the spherical hinge is given by

$$\begin{aligned} N_2 &= 0.7R \times (L_2 - L_1) \\ &= -2.1\mu WR \sin \psi - 0.233\rho\Omega^2 R^4 cC_{L_\alpha}(\theta_{cyc} + \omega_2/\Omega) \\ &\quad + 0.1167\rho\Omega^2 R^4 cC_{L_\alpha} \cdot \\ &\quad \cdot [K_{PC}(\beta_1 - \beta_2) + \tau(\dot{\beta}_1 - \dot{\beta}_2)/\Omega - \Delta\alpha_{g_1} + \Delta\alpha_{g_2}] \end{aligned}$$

The first two terms in the final expression of  $N_2$  match those included in the derivation of the teetering moments discussed in [1], whereas the last term includes the effects of possible aerodynamic load increments induced by a difference in the coning motion of the two blades.

The expression of the aerodynamic moment generated by the paddles around the rotor feathering axis is not affected by the configuration of the coning hinges, and it is written as in [1]. In dimensional terms the expression is

$$N_1 = -0.25\rho\Omega^2 R_{fb}^3 S_{fb} C_{L_{\alpha_{fb}}}(\omega_1/\Omega)$$

## Rotor equations of motion

After introducing the small angle assumption, such that  $\cos \theta_i \approx 1$  and  $\sin \theta_i \approx \theta_i$  with  $\theta_i \in \{\gamma, \beta_0, \beta_1, \beta_2\}$ , and writing all the equations in terms of the relevant vector components, a set of linear ordinary differential equations with periodic coefficients is derived for describing the motion of the central hub and blades, in terms of feathering and teetering degrees of freedom, and coning angles, respectively.

Feathering and teetering dynamics are expressed by the equations

$$\begin{aligned} &[J_{H_F} + J_{F_B} + 2m_{bl}h_C^2] \dot{\omega}_1 = \\ &- [J_{F_B} + (J_{H_P} - J_{H_T}) - 2m_{bl}h_C^2] \omega_2 \Omega + m_{H_F} \\ &[J_{H_T} + 2I_{bl} + 2m_{bl}(r_C^2 + h_C^2) + 4S_{bl}r_C] \dot{\omega}_2 + \\ &(I_{bl} + S_{bl}r_C)(\ddot{\beta}_2 - \ddot{\beta}_1) = - [J_{H_F} - J_{H_P} + \\ &\quad + 2m_{bl}(h_C^2 - r_C^2) - 4S_{bl}r_C - 2I_{bl}] \omega_1 \Omega \\ &\quad - (I_{bl} + S_{bl}r_C)(\beta_2 - \beta_1)\Omega^2 + m_{H_T} \end{aligned}$$

where  $m_{H_F} = N_2 - K\gamma$  and  $m_{H_T} = N_1 - K\beta_0$  are the external aerodynamic and elastic moments acting around the feathering and teetering axes of the spherical joint.

The equations for the relative motion of the blades with respect to the yoke are given by

$$I_{bl}\ddot{\beta}_i \mp (I_{bl} + S_{bl}r_c)\dot{\omega}_2 + (I_{bl} + S_{bl}r_c)(\Omega^2\beta_1 \pm \Omega\omega_1) = m_{C_i}$$

where  $m_{C_i}$  is the total external moment applied around the coning hinge, which may include, together with the aerodynamic term, contributions from elastic, viscous or dry friction terms.

Teetering rotor models are derived from those representing the dynamics of a fully gimbaled one by setting feathering angle and rate,  $\gamma$  and  $\dot{\omega}_1$ , to zero. Freezing the coning degrees of freedom, so that  $\beta_i = \beta_H$  and  $\dot{\beta}_i = 0$ ,  $i = 1, 2$ , the rigid gimbaled rotor analyzed in [1] is recovered.

Finally, a constant rotor angular rate  $\Omega$  is assumed, so that it is possible to transform all the differential equations from the time domain into the angular variable  $\psi$  by means of the chain rule for derivatives, such that  $\dot{x} = dx/dt = (dx/d\psi)(d\psi/dt) = x'\Omega$ . For second order derivatives, it is  $\ddot{x} = x''\Omega^2$ .

### Friction

Due to the centrifugal load, a dry friction of approximately 100 Nm in the coning hinge was considered realistic following some tests. As the effects of friction on rotor dynamics and stability can be significant, a simple friction model is introduced, letting

$$m_{C_i}^{fric} = -k_{fr}\text{sign}(\dot{\beta}_i)$$

where  $k_{fr}$  is a friction coefficient that depends on hinge characteristics and centrifugal force, whereas the sign function is defined as

$$\text{sign}(x) = \begin{cases} 1 & \text{if } x > 0 \\ -1 & \text{if } x < 0 \end{cases}$$

The friction torque is constant in magnitude and opposite with respect to the direction of the coning motion. Note that within this simple friction model, stick-slip phenomena are not taken into account. Moreover, the sudden changes in sign of the friction torque introduce problems for (i) the numerical integration of the equations of motion and (ii) the evaluation of inertial loads, especially when the coning motion is close to an equilibrium and  $\dot{\beta}_i \approx 0$ .

Table 1: Rotor and fuselage parameters

rotor angular rate	$\Omega$	53 rad/s
rotor radius	$R$	3.8 m
blade chord	$c_{bl}$	0.23 m
fly-bar radius	$R_2$	1.45 m
fly-bar root cut-out	$R_1$	1.15 m
paddle chord	$c_{fb}$	0.25 m
blade lift curve slope	$C_{L_\alpha}$	5.7
hub stiffness	$K$	7,219 Nm/rad
pitch hinge stiffness	$K_T$	143 Nm/rad
blade inertia	$I_{bl}$	87.7 kg m <sup>2</sup>
blade static moment	$S_{bl}$	17.7 kg m
blade mass	$m_{bl}$	10.75 kg
fly-bar inertia	$J_{fb}$	5.012 kg m <sup>2</sup>
fuselage mass	$m_f$	650 kg
fuselage parasite area	$C_{D_f}$	5.28 m <sup>2</sup>

A fixed-step integration algorithm was adopted for performing the numerical simulations, with an integration step  $\delta\psi$  that resulted into a reasonable CPU time for the simulations, while maintaining rotor behaviour independent of  $\delta\psi$  itself. At the same time a small "viscous interval" was introduced around the stick condition  $\dot{\beta}_i \approx 0$ , which avoids non-physical high-frequency variations of inertial forces.

### Coupled rotor-fuselage heave motion

In order to investigate rotor loads during gust encounters and the effects of the pitch-coning coupling, a vertical translational degree of freedom for the fuselage is introduced (heave motion). In order to consider all the time-scales relevant to the response, a uniform first order dynamic inflow model was also included in the model, resulting in a 11<sup>th</sup> order system.

Rotor thrust sustains both vehicle's weight and its drag, evaluated by means of an equivalent parasite area. The intensity of the flow impinging on the fuselage is given by the vector sum of helicopter vertical speed and inflow. Inertial coupling between coning motion and fuselage vertical displacement is also significant and it is included in the model.

## Results

In this section the behaviour of the gimbaled rotor is compared to that of an equivalent teetering rotor, with and without the coning degrees of freedom.

Table 2: Eigenvalues for  $K_{PC} = 1.36$  and  $k_{fr} = 0$ .

Gimballed rotor	Teetering rotor
with coning	
$0.1339 \pm 2.3686i$	$0.1254 \pm 2.3545i$
$-0.1871 \pm 1.2464i$	$-0.1871 \pm 1.2460i$
$-0.3745 \pm 0.8357i$	$-0.3758 \pm 0.8605i$
$-0.1263 \pm 0.9642i$	
without coning	
$-0.2170 \pm 0.9740i$	$-0.2179 \pm 0.9760i$
$-0.1187 \pm 0.9623i$	

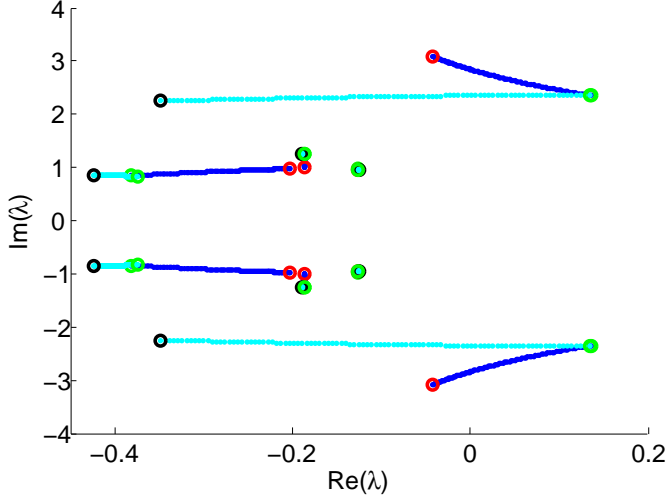


Figure 2: Root loci for the gimballed rotor in hover ( $K_{PC} = 0$  and  $c_{fr} = 0$ :  $\circ$ ;  $0 < K_{PC} < 1.36$  with  $c_{fr} = 0$ :  $\dots$ ;  $K_{PC} = 1.36$  and  $c_{fr} = 0$ :  $\circ$ ;  $0 < c_{fric} < 0.4$  with  $K_{PC} = 1.36$ :  $\dots$ ;  $K_{PC} = 1.36$  and  $c_{fr} = 0.4$ :  $\circ$ ).

The stability of the rotor is analyzed first, for different pitch–coning coupling and in the presence of dry friction in the coning hinges. Response to swashplate commands and gust disturbances are presented to highlight the peculiar behavior of the gimballed rotor.

### Stability analysis

The impact of rotor configuration on rotor stability is here considered, and in particular the presence of coning hinges (CH), their location, pitch–flap coupling coefficient, damping or friction in the hinges. Table 2 collects the eigenvalues in hover of the basic rotor configuration.

While both the gimballed and the teetering rotor without CH are stable, the introduction of the coning degree of freedom with a high pitch–coning coupling leads both configurations to instability. The first os-

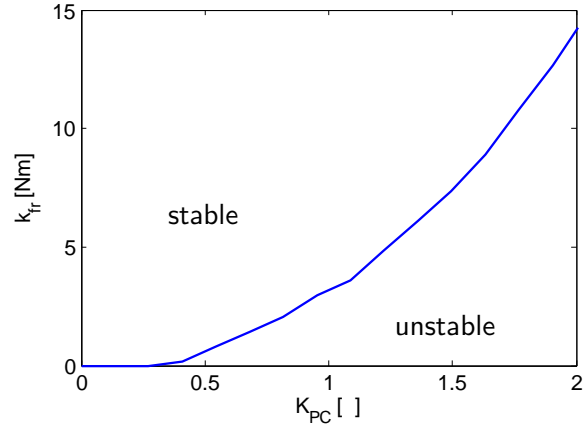


Figure 3: Stability limit in the  $k_{fr}$  vs  $k_{pc}$  plane.

cillatory mode in both the gimballed and teetering rotors is unstable and it excites all states which lies in the plane perpendicular to the coning hinges (i.e.  $\beta_0$ ,  $\beta_1$  and  $\beta_2$ ). This mode is an anti–symmetric coning, where the blades exchange energy through the mechanical link represented by the teetering hub, with coning rotations  $\beta_1$  and  $\beta_2$  of opposite phase and  $\beta_0$  in quadrature.

The rotor becomes stable if the pitch–coning coupling gain is sufficiently reduced and/or some form of dissipation in the coning hinges is introduced. Figure 2 shows the root–loci of when the pitch–coning coupling varies from  $K_{PC} = 0$  to the nominal value,  $K_{PC} = 1.36$  (blue line). The imaginary axis is crossed for  $K_{PC} \approx 0.4$  and the rotor remains unstable for larger values of  $K_{PC}$ . When a viscous damping term proportional to the coning speed ( $M_{vsc_i} = -c_{vsc}\dot{\beta}_i$ ) is introduced for  $K_{PC} = 1.36$ , the system turns stable again, for  $c_{fric} > 0.15$ . On the converse, the feathering mode for the gimballed rotor is always stable and almost unaffected by the presence of coning hinges (the feathering pole,  $-0.1263 \pm 0.9642i$ , being very close to that obtained for blades fixed to the hub,  $-0.1187 \pm 0.9623i$ ) or the introduction of viscous damping (see Fig. 2).

The actual gimballed rotor does not features dampers, yet the high centrifugal load leads to the presence of dry friction in the coning hinges, that dissipates energy. This type of hard nonlinearity prevents the system from being linearized and, as a consequence, a stability analysis based on the eigenvalues is no longer available. Nonetheless, it is possible to identify a minimum value for  $k_{fr}$  which guarantees stability, on the basis of a Poincaré mapping approach: a perturbed state for the rotor is considered as the initial condition and the perturbation after a

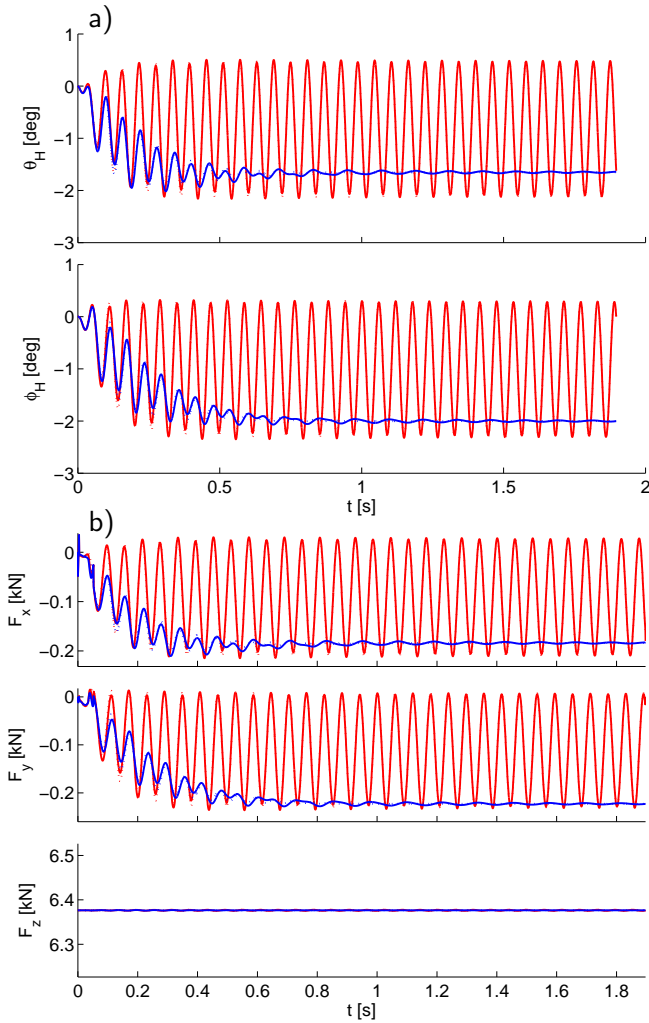


Figure 4: Rotor behavior at  $\mu = 0.1$  with cyclic pitch and no hinge stiffness: a) hub tilt angles ; b) loads transmitted to the shaft. Gimb. rotor with CH (—), gimb. rotor without CH (---), teet. rotor with CH (—), teet. rotor without CH (---)

rotor revolution is evaluated by means of numerical simulation. If the norm of the perturbation after one revolution is smaller than the initial one the rotor is stable. Figure 3 shows the minimum level of friction in the coning hinges in order to guarantee stability as a function of the pitch–coning coupling. The nominal value of the friction  $k_{fr} = 100 \text{ Nm}$  satisfies the stability condition for  $K_{PC} = 1.36$ .

### Isolated rotor response

The behavior of gimballed and teetering rotors with and without CH is compared. The same set of initial conditions is considered in all the simulations, with the vehicle at trim in hover, rotor thrust balancing vehicle's weight and assuming cyclic pitch commands close to zero. A periodic forcing term is introduced

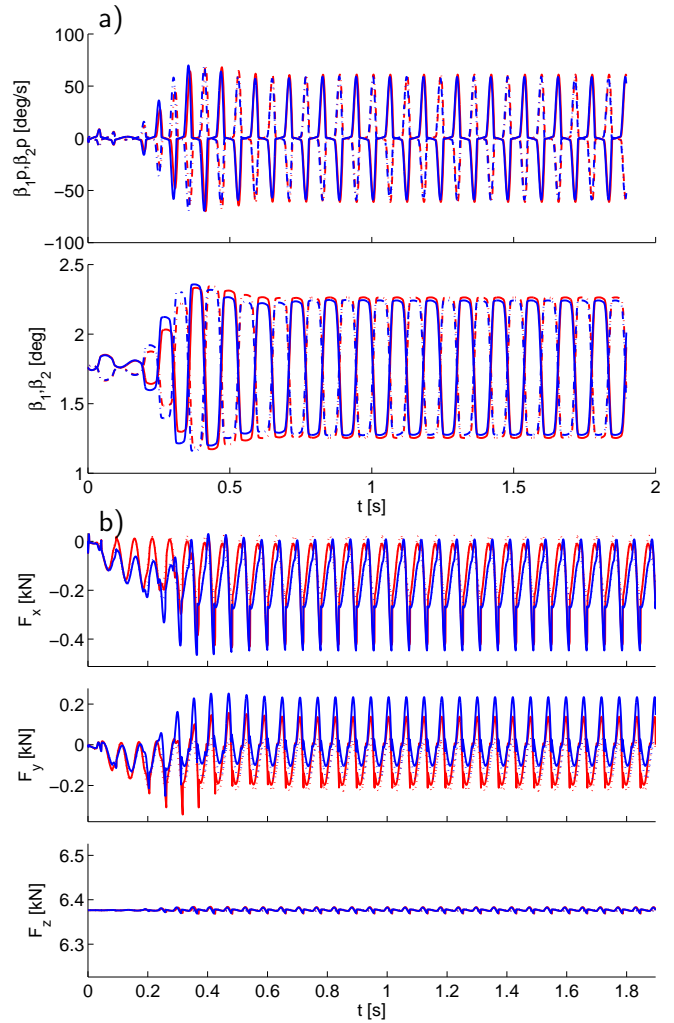


Figure 5: Rotor behavior at  $\mu = 0.1$  with cyclic pitch and hinge stiffness: a) blade coning angles: Gimb. rotor: blade 1 (—) blade 2 (---), Teet. rotor: blade 1 (—) blade 2 (---), b) Force components in shaft axis: Gimb. rotor with CH (—), gimb. rotor without CH (---), teet. rotor with CH (—), teet. rotor without CH (---)

assuming a step variation of advance ratio ( $\mu = 0.1$ ) and cyclic pitch, where the latter command is chosen in order to trim the helicopter at the corresponding speed. Figures 4 reports the resulting behavior of the rotor with dry friction in CH and no stiffness in hub teetering and feathering hinges.

The presence of the feathering degree of freedom allows the gimballed rotor to tilt almost exactly in the direction commanded by the swashplate, if no stiffness is present in the spherical gimbal, a negative value indicating forward tilt. A minor difference between no–feathering–plane and tip–path–plane is present, due to the aerodynamic periodic term.

The hub tilt angle, seen in the non–rotating frame,

presents oscillations of small amplitude. As a consequence the in-plane rotor load oscillations (aerodynamic and inertial force components perpendicular to the shaft axis) remain small. On the converse, the teetering rotor presents a more intense oscillation. The presence of CH in both the gimbaled and teetering rotor leads to marginal variations in the behaviour of the system.

When a stiffness  $K = 7219 \text{ Nm/rad}$  is introduced in hub teetering and feathering hinges, the gimbaled rotor is no longer capable of tilting the hub exactly in the direction of the no-feathering-plane (Fig. 5), an equilibrium condition being no longer available, as discussed in [1]. Both hub and blades present a periodic behaviour. The shape of the oscillations of coning angles and rates is a consequence of the friction in the coning hinges, with intervals during which friction keeps  $\dot{\beta}_i$  close to zero (stick phase). As for the rest, the behaviour resembles that of the rigid rotor with cantilevered blades considered in [1]. The impact of CH in the case of response to commands and loads transmitted in forward flight is thus limited.

### Gust response

The presence of CH and pitch-coning coupling is motivated by a better gust response which should limit the peak load transmitted to the fuselage during a gust encounter, and provide inherent stability to the rotor, as discussed in [6]. In this respect, the rigid blade model considered in [1] penalizes the configuration with no CH, as blade flexibility and torsional deformation would induce a significant coupling between local incidence and effective blade coning.

Figure 6 describes the behavior of a rotor in hover with longitudinal cyclic pitch which experiences a severe vertical gust. In the first 0.6 s the rotor responds to the  $5^\circ$  longitudinal cyclic command. The tip-path-plane of all rotor configurations (evaluated for  $\psi = 0, \pi$  for  $a_1$  and for  $\psi = \pi/2, 3\pi/2$ ) tilts in the same direction of the swashplate. Rotors with coning hinges presents a longer settling time before reaching the equilibrium value due to the blade coning motion.

During gust penetration both blades move upwards and the coning angle  $a_0$  reaches a higher equilibrium position, when an inertially fixed isolated rotor is considered. At the same time the pitch-coning coupling reduces the steady state value of the rotor vertical forces, if compared with a rotor with no CH.

### Gust response with heave motion

Figure 7 compares the gust response in hovering for

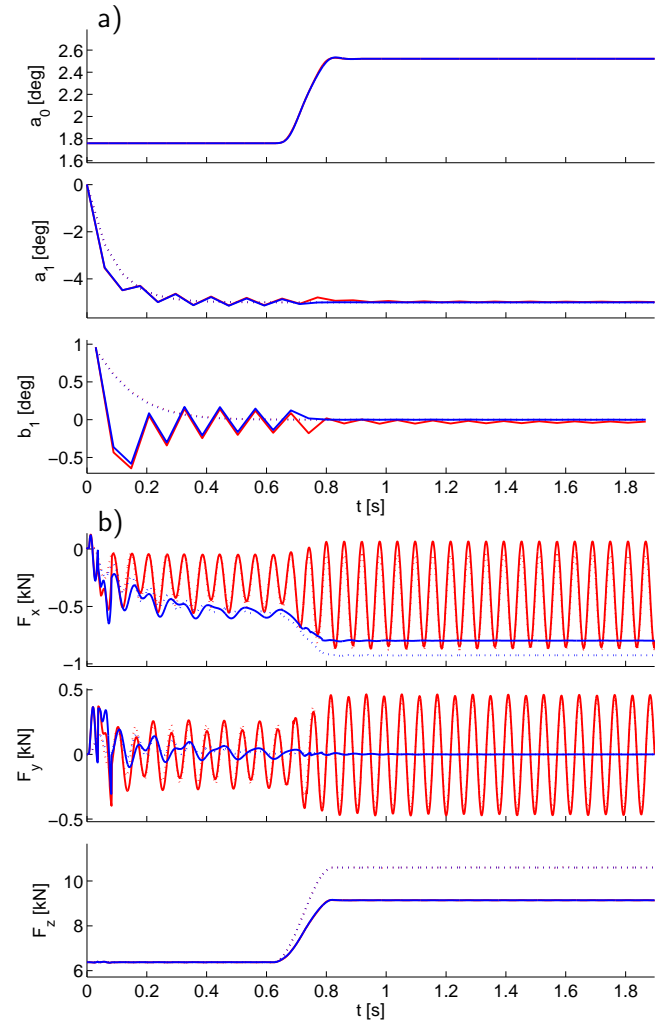


Figure 6: Rotor response to a step gust at  $t = 0.6 \text{ s}$  in hover with  $5^\circ$  longitudinal cyclic: a) TPP states; b) loads transmitted to the shaft. Gimbaled rotor with CH (—), gimbaled rotor without CH (···), teetering rotor with CH (—), teetering rotor without CH (···)

an isolated rotor with that obtained for the simplified fuselage-rotor model, featuring a vertical translational degree of freedom, described at the end of the Section on “Rotor Models”. In both cases a fully gimbaled rotor is considered.

When fuselage heave motion is included in the model, the helicopter accelerates in the direction of the gust as shown in Fig. 8. The relative speed of the helicopter with respect to the surrounding air mass reduces the variation of the angle of attack generated by the gust.

The gimbaled rotor with CH presents a better gust response from both an aerodynamic and a dynamic standpoint. On one side, the variation of pitch angle induced by the pitch-coning coupling reduces the angle-of-attack variation and, as a direct conse-

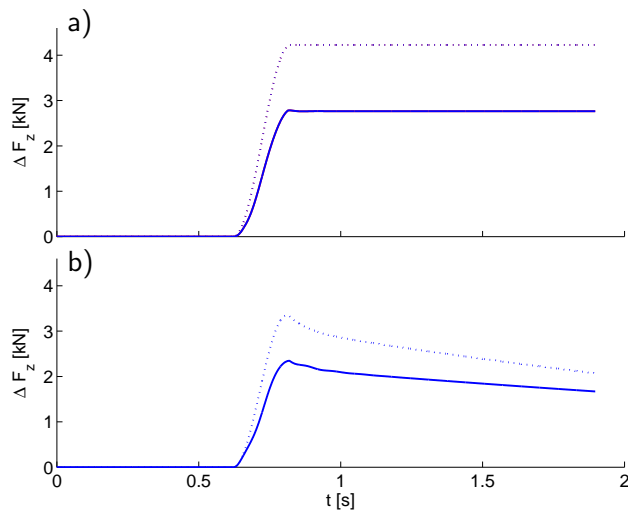


Figure 7: Rotor thrust response to a 0.2 s gust: a) rotor only; b) rotor and fuselage heave motion. Hover without cyclic pitch and no stiffness in rotor hub. Rotor with friction and  $K_{PC} = 1.36$  (—), rotor without coning (···).

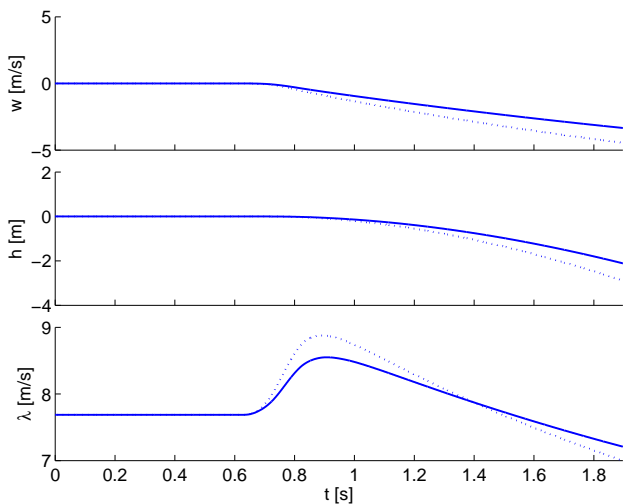


Figure 8: Fuselage and inflow states response to 0.2 s step gust. Rotor with friction and  $K_{PC} = 1.36$  (—), rotor without coning (···).

quence, the peak load. At the same time, the vertical load on the fuselage is reduced, when part of the aerodynamic load excites the coning response.

## Conclusions

The characteristics of a two-bladed gimballed rotor featuring a homokinetic joint between driving shaft and rotor yoke, fly-bar with paddles and coning hinges were analyzed. A simplified model based on the as-

sumption of small angles and aerodynamic load concentrated at 70% of the blade span was developed.

The presence of coning hinges and a high pitch-coning coupling makes the system unstable. The rotor is stabilized by a sufficient amount of dissipation, due to either viscous damping or dry friction in coning hinges. In this respect, the friction generated in the coning hinges by the high centrifugal load is sufficient to this end in all considered flight conditions.

Command and gust response of gimballed and teetering rotors with and without coning hinges were compared. The presence of the coning degrees of freedom has a marginal effect on both the gimballed and teetering rotors response to commands and steady state behaviour. On the converse, coning hinges provide a significant load alleviation during gust encounters, an effect which is increased when a pitch-coning coupling mechanism is included.

## References

1. Avanzini, G., de Matteis, G., Lucertini F., and Torasso A., "Dynamic Behaviour and Response of a Two-Bladed Gimballed Rotor." 36th European Rotorcraft Forum, Paris, France, 7-9 September 2010.
2. Chaplin, H.R., "Some Dynamic Properties of a Rigid Two-Bladed Fully Gimballed Tip-Jet Helicopter Rotor with Circulation Control", TM-16-80/16, D.W. Taylor Naval Ship Research and Development Center, Bethesda (MD), USA, August 1980.
3. Chen, R.T.N., "A Simplified Rotor System Mathematical Model for Piloted Flight Dynamics Simulation", NASA TM 78575, Ames Research Center, Moffett Field (CA), USA, May 1979.
4. Ferri, R., "Analisi dinamica di un rotore teetering con cerniere di conicit ," Master Thesis, "Sapienza" Universit  di Roma, Rome, 2011 (in Italian).
5. Chaplin, H.R., "Some Dynamic Properties of a Rigid Two-Bladed Fully Gimballed Rotor with Teetering Feedback", TM-16-86/02, D.W. Taylor Naval Ship Research and Development Center, Bethesda (MD), USA, July 1986.
6. Hohenemser, K., "A Type of Lifting Rotor with Inherent Stability," J. Aeron. Sc., Vol. 17, September 1950, pp. 555-563.
7. Marks, M.D., "Comparison of Current Operational Rotor Systems and a Rotor Having Floating Hub and Offset Coning Hinges," J. Am. Helic. Soc., Vol. 5, No. 4, October 1960, pp. 13-24.
8. Bramwell, A.R.S., *Helicopter Dynamics*, 2nd edition, Butterworth-Heinemann, Oxford, 2001.